

Weakly-supervised Action Localization with Background Modeling

Phuc Xuan Nguyen
University of California, Irvine
nguyenpx@ics.uci.edu

Deva Ramanan
Carnegie Mellon University
deva@cs.cmu.edu

Charless C. Fowlkes
University of California, Irvine
fowlkes@ics.uci.edu

Abstract

We describe a latent approach that learns to detect actions in long sequences given training videos with only whole-video class labels. Our approach makes use of two innovations to attention-modeling in weakly-supervised learning. First, and most notably, our framework uses an attention model to extract both foreground and background frames whose appearance is explicitly modeled. Most prior works ignore the background, but we show that modeling it allows our system to learn a richer notion of actions and their temporal extents. Second, we combine bottom-up, class-agnostic attention modules with top-down, class-specific activation maps, using the latter as form of self-supervision for the former. Doing so allows our model to learn a more accurate model of attention without explicit temporal supervision. These modifications lead to 10% $AP@IoU=0.5$ improvement over existing systems on THUMOS14. Our proposed weakly-supervised system outperforms recent state-of-the-arts by at least 4.3% $AP@IoU=0.5$. Finally, we demonstrate that weakly-supervised learning can be used to aggressively scale-up learning to in-the-wild, uncurated Instagram videos. The addition of these videos significantly improves localization performance of our weakly-supervised model.

1. Introduction

We explore the problem of weakly-supervised action localization, where the task is learning to detect and localize actions in long sequences given videos with only video-level class labels. Such a formulation of action understanding is attractive because it is well-known that precisely estimating the start and end frames of actions is challenging even for humans [3]. We build on a body of work that makes use of attentional processing to infer frames most likely to belong to an action. We specifically introduce the following innovations.

Background modeling: Classic pipelines use attentional pooling to focus a model on those frames likely to

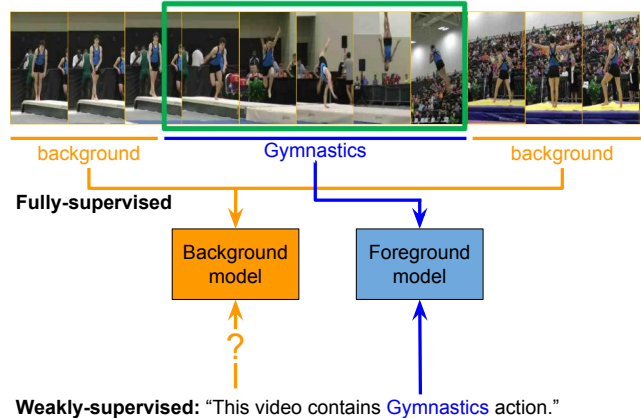


Figure 1: With fully-supervised data where exact boundaries of actions are provided, we can train highly discriminative detection models that use background regions as negative examples, implicitly modeling background content. In weakly-supervised setting where only video-level labels are known, current approaches simply train a foreground model to respond strongly at some locations within the video, but leave the remaining background frames unmodeled. In this paper we show that a model which explicitly accounts for background frames substantially improves on weakly-supervised localization.

contain the action of interest. We show that by modeling the remaining background frames, one can significantly improve the accuracy of such methods. Interestingly, fully-supervised systems for both objects [22] and actions [4] tend to build explicit models (or classifiers) for background patches and background frames, but this type of reasoning is absent in most weakly-supervised systems. Notable exceptions in the literature include probabilistic latent-variable models that build generative models of both foreground and background [16]. We incorporate background modeling into discriminative network architectures as follows: many such networks explicitly compute an attention variable, λ_t , that specifies how much frame t should influence the final video-level representation (by say, weighted pooling across all frames). Simply put, we construct a pooled video-level feature that focuses on the background by weighing frames

with $1 - \lambda_t$.

Top-down guided attention: Our second innovation is the integration of top-down attentional cues as additional forms of supervision for learning bottom-up attention. The attention variable λ_t , typically class-agnostic, looks for generic cues that apply to all types of actions. As such, it can be thought of as a form of bottom-up attentional saliency [9]. Recent works have shown that one can also extract *top-down* attentional cues from classifiers that operate on pooled features by looking at (temporal) class activation maps (T-CAM) [19, 38]. We propose to use class-specific attention maps as a form of supervision to refine the bottom-up attention maps λ_t . Specifically, our loss encourages bottom-up attention maps to agree with top-down class-specific attention map (for classes *known* to exist in a given training video).

Micro-videos as training supplements: We observe there is a huge influx of microvideos on social media platforms (Instagram, Snapchat) [20]. These videos often come with user-generated tags, which can be loosely viewed as video-level labels. This type of data appears to be an ideal source for weakly-supervised video training data. However, the utility of these videos remains to be established. In this paper, we show that the addition of microvideos to existing training data allows aggressive scaling up of learning which improves action localization accuracy.

Our contributions are summarized below:

- We extend prior weakly-supervised action localization systems to include background modeling and top-down class-guided attention.
- We present extensive comparative analyses between our models versus other state-of-the-art action localization systems, both weakly-supervised and fully-supervised, on THUMOS14 [15] and ActivityNet [13].
- We demonstrate the promising effects of using microvideos as supplemental, weakly-supervised training data.

2. Related Works

In recent years, progress in temporal action localization has been driven by large-scale datasets such as THUMOS14 [15], Charades [27], ActivityNet [13] and AVA [12]. Building such datasets has required substantial human effort to annotate the start and end points of interesting actions within longer video sequences. Many approaches to fully-supervised action localization leverage these annotations and adopt a two-stage, propose-then-classification framework [2, 26, 7, 14, 24, 37]. More recent state-of-the-art methods [11, 10, 32, 5, 4] borrow intuitions from the recent object detection frameworks (e.g. R-CNN). One common factor among these approaches is

using non-action frames within the video for building background model.

Temporal boundary annotations, however, are expensive to obtain. This motivates efforts in developing models that can be trained with weaker forms of supervision such as video-level labels. UntrimmedNets [30] uses a classification module to perform action classification and selection module to detect important temporal segments. Hidden-Seek [29] addresses the tendency of popular weakly-supervised solutions - networks with global average pooling - to only focus on the most discriminative frames by randomly hiding parts of the videos. STPN [19] introduced an attention module to learn the weights for the weighted temporal pooling of segment-level feature representations. This method generates detections by thresholding Temporal Class Activation Mappings (T-CAM) weighted by the attention values. AutoLoc [25] introduces a boundary predictor to predict segment boundaries using an anchoring system. The boundary predictor is driven by the Outer-Inner-Contrastive Loss, which encourages segments with high activation on the inside and weaker activations on the immediate neighborhood of this segment. W-TALC [21] introduces a system with k-max Multiple Instance Learning and explicitly identifies the correlations between videos of similar categories by a co-activity similar loss. None of the aforementioned methods attempts to explicitly model background content during training.

3. Localization from Weak Supervision

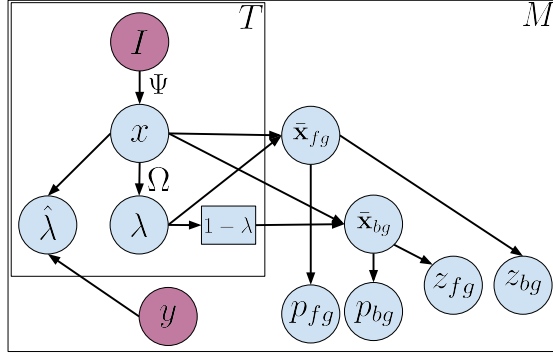
Assume we are provided with a training set of videos and video-level labels $y \in \{0, \dots, C\}$, where C denotes the number of possible actions and 0 indicates no action (the background). In each frame t of each video, let us write $\mathbf{x}_t \in \mathbb{R}^d$ for a feature vector based on RGB and optical flow extracted at that frame (e.g., pretrained on a related video classification task). We then can write each training video as a tuple of feature vectors and video-level label:

$$(\{\mathbf{x}_t\}, y), \quad \mathbf{x}_t \in \mathbb{R}^d, y \in \{0, \dots, C\}$$

In principle, videos may contain multiple types of actions, in which case it is more natural to model y as a multi-label vector. From this set of *video-level* training annotations, our goal is to learn a *frame-level* classifier that can identify which of the $C + 1$ actions (or background) is taking place at each frame of a test video.

3.1. Weak Supervision

To produce video-level predictions of foreground actions, we perform attention-weighted average pooling of frame features over the whole video to produce a single



$$||\lambda - \hat{\lambda}||_1 - \log p_{fg}[y] - \log p_{bg}[0] - \log z_{fg} - \log z_{bg}$$

self-guided loss
foreground class loss
background class loss
cluster loss

Figure 2: Network architecture for our weakly supervised action localization model. Using a pre-trained network, we extract the features representation for short video segments. The attention module Ω predicts frame level attention λ which can be used to pool the frame-level features into a single foreground video-level feature representation. The complement of the attention vector, $1 - \lambda$, can also be used to pool segments belonging to the background into a video-level background representation. Video-level labels are predicted from these pooled features. In addition to this action-specific top-down model appearance, we also include bottom-up clustering loss which asserts that the video should segment into distinct foreground and background appearances z_{fg}, z_{bg} . To link these two, we compute an attention target $\hat{\lambda}$ based on the class activations of the ground-truth video label y using a “self-guided” loss that encourages the predicted attention λ to match this target.

video-level *foreground* feature \mathbf{x}_{fg} given by

$$\mathbf{x}_{fg} = \frac{1}{T} \sum_{t=1}^T \lambda_t \mathbf{x}_t. \quad (1)$$

The weighting for each frame is a scalar $\lambda_t \in [0, 1]$ which serves to pick out (foreground) frames during which an action is taking place while down-weighting contribution from background. The attention is a function of the d -dimensional frame feature $\lambda_t = \Omega(x_t)$ which we implement using two fully-connected (FC) layers with a ReLU activation for the first layer and a sigmoid activation function for the second.

To produce a video-level prediction, we feed the pooled feature to fully-connected softmax layer, parameterized by $w_c \in \mathbb{R}^d$ for class c :

$$p_{fg}[c] = \frac{e^{w_c \cdot \mathbf{x}_{fg}}}{\sum_{i=0}^C e^{w_i \cdot \mathbf{x}_{fg}}} \quad (2)$$

The foreground classification loss is the defined via regular cross-entropy loss with respect to the video label y .

$$\mathcal{L}_{fg} = -\log p_{fg}[y] \quad (3)$$

Background-Aware Loss The complement of the attention factor, $1 - \lambda$, indicates frames where the model believes that no action is taking place. We propose that features pooled from such background frames \mathbf{x}_{bg} should also be classified by the *same* softmax model as was applied to the pooled foreground frames.

$$\mathbf{x}_{bg} = \frac{1}{T} \sum_{t=1}^T (1 - \lambda_t) \mathbf{x}_t \quad (4)$$

$$p_{bg}[c] = \frac{e^{w_c \cdot \mathbf{x}_{bg}}}{\sum_{i=0}^C e^{w_i \cdot \mathbf{x}_{bg}}} \quad (5)$$

The vector, $p_{bg} \in \mathbb{R}^{C+1}$, indicate the likelihood of each action class for the background-pooled features. The background-aware loss, \mathcal{L}_{bg} , encourages this vector to be close to 1 at the background index, $y = 0$, and 0 otherwise. This cross entropy loss on the background feature then simplifies to

$$\mathcal{L}_{bg} = -\log p_{bg}[0]$$

Compared to a model which is trained to classify only foreground frames, \mathcal{L}_{bg} , ensures that the parameters w also learn to distinguish actions from the background.

Self-guided Attention Loss The attention variable λ_t can be thought of as a *bottom-up*, or class-agnostic, attention model that estimates the foreground probability of a frame. This will likely respond to generic cues such as large body motions, which are not specific to particular actions. Recent works have shown one can extract *top-down* attentional cues from classifiers operating on pooled features by examining (temporal) class activation maps (TCAM) [19, 38]. We propose to use class-specific TCAM attention maps as a form of self-supervision to refine the class-agnostic bottom-up attention maps λ_t . Specifically, we use top-down attention maps from the class y that is *known* to be a given training video:

$$\hat{\lambda}_t^{fg} = G(\sigma) * \frac{e^{w_y \mathbf{x}_t}}{\sum_{i=0}^C e^{w_i \mathbf{x}_t}} \quad (6)$$

where $G(\sigma)$ refers to a Gaussian filter used to temporally smooth the class-specific, top-down attention signals.¹ Gaussian smoothing imposes the intuitive prior that if a frame has high probability of being an action, its neighboring frames should also have high probability of containing an action. Note the above softmax differs from (2) and (5) in that they are defined at the frame level (as opposed to the video level) and that they are **not** modulated by bottom-up attention $\lambda_t = \Omega(\mathbf{x}_t)$.

¹If video is labeled with multiple actions, we max-pool foreground attention targets $\hat{\lambda}_t^{fg}$ across all present actions so that $\hat{\lambda}_t$ is large if any action is taking place at time t .

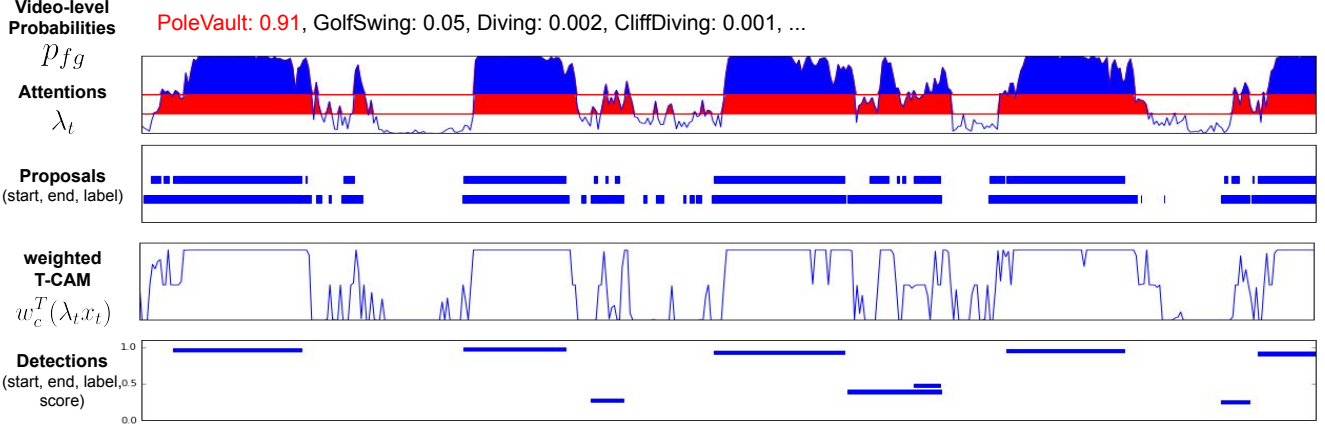


Figure 3: The detection process involves three steps: video-level class probability thresholding, segment proposal generation and detection scoring. First, relevant classes are selected by thresholding video-level probabilities. The attention vector is thresholded with different values to select salient, connected segments. Each threshold value corresponds to a different set of segment proposals which are pooled. Each proposal is scored by averaging the weighted-TCAM values within its interval. Per-class non-maxima suppression is performed to remove highly overlapped detections. The y-axis in last figure indicates the final detection score.

Since our top-down classifier also includes a model of background, we can consider an attention target given by the complement of the background class activations

$$\hat{\lambda}_t^{\text{bg}} = G(\sigma) * \frac{\sum_{i=1}^C e^{w_i \mathbf{x}_t}}{\sum_{i=0}^C e^{w_i \mathbf{x}_t}} \quad (7)$$

Given this attention target, we define the self-guided loss as

$$\mathcal{L}_{\text{guide}} = \frac{1}{T} \sum_t |\lambda_t - \hat{\lambda}_t^{\text{fg}}| + |\lambda_t - \hat{\lambda}_t^{\text{bg}}|$$

which biases the class-agnostic bottom-up attention map to agree with the top-down class-specific attention map (for classes known to exist in a given training video).

Foreground-background Clustering Loss Finally, we consider a bottom-up loss defined purely in terms of the video features and attention λ which makes no reference to the video-level labels. We estimate another set of parameters $u_{fg}, u_{bg} \in \mathbb{R}^d$ that are applied to the bottom-up attention-pooled features (that do not require top-down class labels)

$$z_{\text{fg}} = \frac{e^{u_{fg} \mathbf{x}_{fg}}}{e^{u_{fg} \mathbf{x}_{fg}} + e^{u_{bg} \mathbf{x}_{fg}}} \quad (8)$$

$$z_{\text{bg}} = \frac{e^{u_{bg} \mathbf{x}_{bg}}}{e^{u_{fg} \mathbf{x}_{bg}} + e^{u_{bg} \mathbf{x}_{bg}}} \quad (9)$$

Each video should contain both foreground and background frames so the clustering loss encourages both classifiers respond strongly to their corresponding pooled features

$$\mathcal{L}_{\text{cluster}} = -\log z_{\text{fg}} - \log z_{\text{bg}} \quad (10)$$

This can be viewed as a clustering loss that encourages the foreground and background pooled features to be distinct from each other.

Total loss We combine these losses to yield a total per-video training loss

$$\mathcal{L}_{\text{total}} = \mathcal{L}_{\text{fg}} + \alpha \mathcal{L}_{\text{bg}} + \beta \mathcal{L}_{\text{guide}} + \gamma \mathcal{L}_{\text{cluster}}. \quad (11)$$

with α, β and γ are the hyperparameters to control the corresponding weights between the losses. We find that these hyperparameters (α, β, γ) need to be small enough so that network is driven mostly by the foreground loss, \mathcal{L}_{fg} .

3.2. Action Localization

To generate action proposals and detections, we first identify relevant action classes based on video-level classification probabilities, p_{fg} . Segment proposals are generated for each relevant class. These proposals are then scored with the corresponding weighted T-CAMs to obtain the final detections. We keep segment-level features at timestamp t with attention value λ_t greater than some pre-determined threshold. We perform 1-D connected components for connect neighboring segments to form segment proposal. A segment proposal $[t_{\text{start}}, t_{\text{end}}, c]$, is then scored as

$$\sum_{t=t_{\text{start}}}^{t_{\text{end}}} \frac{\theta \lambda_t^{\text{RGB}} w_c^T \mathbf{x}_t^{\text{RGB}} + (1 - \theta) \lambda_t^{\text{FLOW}} w_c^T \mathbf{x}_t^{\text{FLOW}}}{t_{\text{end}} - t_{\text{start}} + 1} \quad (12)$$

where θ is a scalar denoting the relative importance between the modalities. In this work, we set $\theta = 0.5$.

Figure 3 shows an example of the inference process. Unlike STPN, we do not generate proposals using attention-

Table 1: Ablation studies show each additional loss leads to significant localization performance gain. The losses also complement each other as combining them achieves better results. The first and second rows are obtained from STPN [19].

\mathcal{L}_{fg}	\mathcal{L}_{bg}	\mathcal{L}_{guide}	$\mathcal{L}_{cluster}$	\mathcal{L}_{sparse}	AP@IoU								
					0.1	0.2	0.3	0.4	0.5	0.6	0.7	0.8	0.9
✓	–	–	–	–	46.6	38.7	31.2	22.6	14.7	–	–	–	–
✓	–	–	–	✓	52.0	44.7	35.5	25.8	16.9	9.9	4.3	1.2	0.2
✓	–	✓	–	–	53.8	46.4	38.2	29.0	19.2	10.6	4.4	1.3	0.1
✓	✓	–	–	–	53.6	47.6	39.1	30.2	20.5	12.2	5.4	1.7	0.2
✓	✓	✓	–	–	58.9	54.3	41.5	33.9	24.4	16.2	7.8	2.4	0.4
✓	✓	–	✓	–	54.9	48.4	40.8	32.4	23.1	14.2	7.4	2.5	0.3
✓	–	✓	✓	–	60.1	54.1	45.6	34.0	23.2	13.6	6.2	1.4	0.1
✓	✓	✓	✓	–	60.4	56.0	46.6	37.5	26.8	17.6	9.0	3.3	0.4

weighted T-CAMs but from the attention vector, λ . Multiple thresholds are used to provide a larger pool of proposals. We find that generating proposals from the averaged attention weights from different modalities leads to more reliable proposals. Class-wise non-maxima suppression (NMS) is used to remove detections with high overlap.

4. Experiments

4.1. Datasets and Evaluation Method

Datasets We evaluate the proposed algorithm on two popular action detection benchmarks, THUMOS14 [15] and ActivityNet1.3 [13].

THUMOS14 has temporal boundary annotations for 20 action classes in 212 validation videos and 200 test videos. Following standard protocols, we train using the validation subset without temporal annotations and evaluate using test videos. Video length ranges from a few seconds up to 26 minutes, with the mean duration around 3 minutes long. On average, there are 15 action instances per video. There is also a large variance in the length of an action instance, from less than a second to minutes.

The ActivityNet dataset offers a larger benchmark for complex action localization in untrimmed videos. We use ActivityNet1.3, which has 10,024 videos for training, 4,926 for validation, and 5,044 for testing with 200 activity classes. For fair comparisons, we use the same pre-extracted I3D features as STPN.

Microvideos are short, untrimmed video clips available on social media platforms, such as Instagram and Snapchat. These videos are authored to be exciting, and hence often have much higher foreground/background content ratio than regular videos. We aim to leverage this new source of data and its accompanying tags to improve action localization performance. We download 100 most-recent Instagram videos containing tags constructed from THUMOS14’s action names. For example, for ‘*BaseballPitch*’, we query Instagram for videos with tag #*baseballpitch*. Duplicated and mis-tagged videos are removed. The retention rate depends on the action labels, ranging from 15% to 89% with

the average retention rate at 45%. It takes less than 2 hours to curate video-level labels for 2000 videos. The final set contains a total of 915 microvideos. The duration for these videos ranges from 6 to 15 seconds. Each video often 1-2 action instances. Example microvideos are shown in our supplementary materials. In our experiments, we simply add these microvideos to the THUMOS14 train set and keep the rest of the experiment unchanged.

We follow the standard evaluation protocol based on mean Average Precision (mAP) values at different levels of intersection over union (IoU) thresholds. The evaluation is conducted using the benchmarking code for the temporal action localization task provided by ActivityNet².

4.2. Implementation Details

For fair comparisons, experiment settings are kept similar to STPN [19]. Specifically, we use two-stream I3D networks trained on Kinetics [17] as segment-level feature extractor. I3D features are extracted using publicly-available code and models³. We follow the preprocessing steps for RGB and optical flow recommended by the software. For the flow stream, we use an OpenCV implementation to calculate the dense optical flow using the Gunnar Farneback’s algorithm [8]. Instead of sampling a fixed number of segments per video like STPN, we load all the segments for one video and process only one video per batch.

The loss function weights in Eq. 11 are set as $\alpha = \beta = \gamma = 0.1$. This specific setting is provided for ease of reproducibility. However, as long as these values are around 10x smaller than foreground class loss weight, converged models have similar performance. Intuitively, video-level labels provide the most valuable supervision. The higher foreground class loss weight encourages the model to first produce correct video-level labels. Once the foreground loss is saturated, minimizing the other losses improves boundary decisions between foreground and background.

The network is implemented in TensorFlow and trained

²<https://github.com/activitynet/ActivityNet/blob/master/Evaluation/>

³<https://github.com/deepmind/kinetics-i3d>

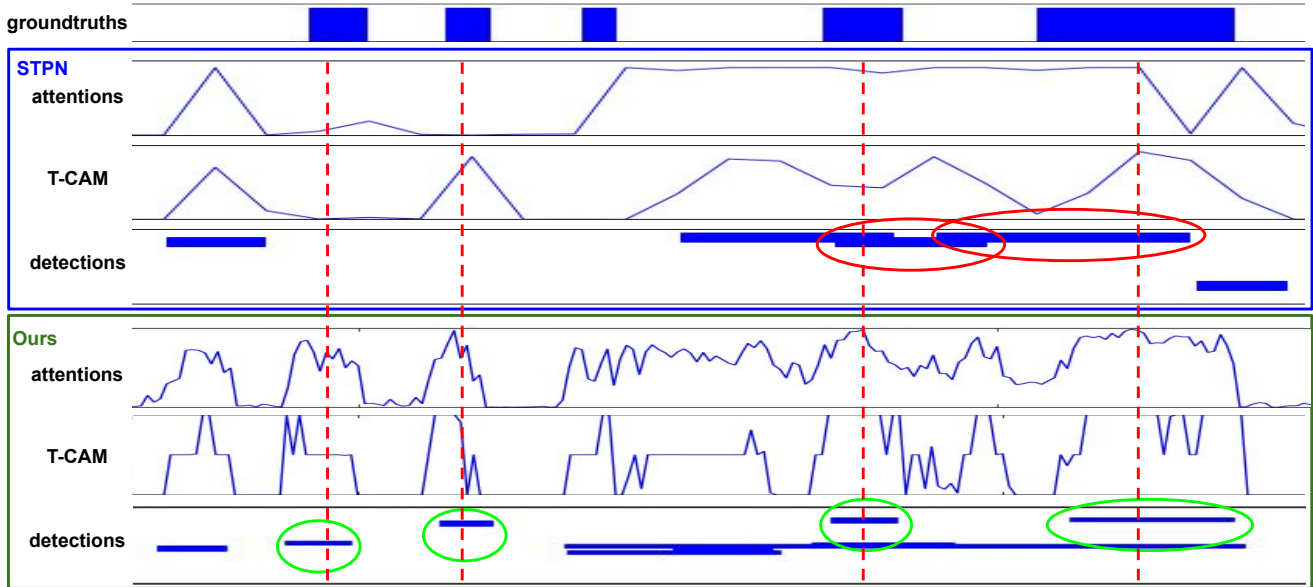


Figure 4: With background modeling, our model is able to produce better attention weights, T-CAM signals and subsequently better detections. The first two action instances (green ellipses) are detected by our methods but completely missed by STPN. While both algorithms detect the last two action instances (last red and green ellipses), ours is able to obtain more accurate boundaries.

using the Adam optimizer with learning rate 10^{-4} . At testing time, we reject classes whose video-level probabilities are below 0.1. If no foreground class has probability great than 0.1, we generate proposals and detections for the highest foreground class. We propose using a large set of thresholds ranging from 0 to 0.5 with the 0.025 increment. All proposals are combined in one large set. We use an NMS overlap threshold of 0.5.

5. Results

We perform ablation studies on different combinations of loss terms to further understand the contribution of each loss. Results in Table 1 suggest the addition of each loss improves localization performance. Combining these losses in training leads to even better results, implying that each provides complementary cues.

Figure 4 shows an example comparing the intermediate outputs between our model and STPN. Our model is able to produce better attentions, T-CAMs, and, consequently, better action detections. Our model is able to detect instances that are completely missed by the previous model. This leads to an overall improvement in the recall rate and average precision of the localization model across different IoU overlap thresholds. For action instances detected by both models, our model is able to obtain more accurate temporal boundaries. This leads to AP improvements for stricter IoU overlap thresholds.

Comparisons with state-of-the-art Table 2 compares the action localization results of our approach on THUMOS14

to other weakly-supervised and fully-supervised localization systems published in the last three years. For IoUs less than 0.5, we improve mAP by 10% mAP over STPN [19]. We also significantly outperform more recent state-of-the-art weakly-supervised action localization systems. Our model is also comparable to other fully-supervised systems, especially in the lower IoU regime. In higher IoU overlap regimes, our model doesn't perform as well as Chao *et al.* [4]. This suggests that our model knows where actions happen, but is not able to precisely articulate the boundaries as well as fully-supervised methods. This is reasonable as our weakly-supervised models are not privy to boundary annotations for which fully-supervised methods have full access.

Table 3 compares our results against other state-of-the-art approaches on the ActivityNet 1.3 validation set. Similar to THUMOS14, our method significantly outperforms existing weakly-supervised approaches while maintaining competitive with other fully-supervised methods.

Micro-videos as supplemental training data Even though THUMOS14 has a uniform number of training videos across each action class, the class distribution of action instances is heavily skewed (ranging from 30 instances of *BaseballPitch* to 499 instances of *Diving*). As a result, categories with higher instance count (*Diving*, *HammerThrow*) have higher mAP while those with fewer action instances (*BaseballPitch*, *TennisSwing*, *CleanAndJerk*) have lower mAP. The addition of microvideos re-balances the skewed class distribution for action instances and improves the gen-

Table 2: Comparisons with recent techniques on THUMOS14. Our method yields 10% improvement over the original system [19]. We significantly outperform other weakly supervised approaches [25, 21], 5% mAP@0.5. In general, our model performance is comparable to fully-supervised methods in lower IoU regimes. Higher IoU requires more accurate action boundary decisions, which is difficult to do without the actual boundary supervision.

Supervision	Method	AP@IoU								
		0.1	0.2	0.3	0.4	0.5	0.6	0.7	0.8	0.9
Fully supervised	Heilbron et al. [14]	–	–	–	–	13.5	–	–	–	–
	Richard et al. [23]	39.7	35.7	30.0	23.2	15.2	–	–	–	–
	Shou et al. [26]	47.7	43.5	36.3	28.7	19.0	10.3	5.3	–	–
	Yeung et al. [34]	48.9	44.0	36.0	26.4	17.1	–	–	–	–
	Yuan et al. [35]	51.4	42.6	33.6	26.1	18.8	–	–	–	–
	Escordia et al. [6]	–	–	–	–	13.9	–	–	–	–
	Shou et al. [24]	–	–	40.1	29.4	23.3	13.1	7.9	–	–
	Yuan et al.[36]	51.0	45.2	36.5	27.8	17.8	–	–	–	–
	Xu et al.[32]	54.5	51.5	44.8	35.6	28.9	–	–	–	–
	Zhao et al. [37]	66.0	59.4	51.9	41.0	29.8	–	–	–	–
	Chao et al. [4]	59.8	57.1	53.2	48.5	42.8	33.8	20.8	–	–
Alwassel et al. [1]	–	–	51.8	42.4	30.8	20.2	11.1	–	–	
Weakly supervised	Wang <i>et al.</i> [30]	44.4	37.7	28.2	21.1	13.7	–	–	–	–
	Singh & Lee [29]	36.4	27.8	19.5	12.7	6.8	–	–	–	–
	Nguyen <i>et al.</i> [19]	52.0	44.7	35.5	25.8	16.9	9.9	4.3	1.2	0.2
	Paul <i>et al.</i> [21]	55.2	49.6	40.1	31.1	22.8	–	7.6	–	–
	Shou et al.[25]	–	–	35.8	29.0	21.2	13.4	5.8	–	–
	Ours	60.4	56.0	46.6	37.5	26.8	17.6	9.0	3.3	0.4
	Ours + MV	64.2	59.5	49.1	38.4	27.5	17.3	8.6	3.2	0.5

Table 3: Results on the ActivityNet1.3 validation set.

	Method	AP@IoU		
		0.5	0.75	0.95
Fully supervised	Singh & Cuzzolin [28]	34.5	–	–
	Wang & Tao [31]	45.1	4.1	0.0
	Shou <i>et al.</i> [24]	45.3	26.0	0.2
	Xiong <i>et al.</i> [37]	39.1	23.5	5.5
	Montes <i>et al.</i> [18]	22.5	–	–
	Xu <i>et al.</i> [33]	26.8	–	–
	Chao <i>et al.</i> [4]	38.2	18.3	1.30
Weakly supervised	Nguyen et al. [19]	29.3	16.9	2.6
	Ours	36.4	19.2	2.9

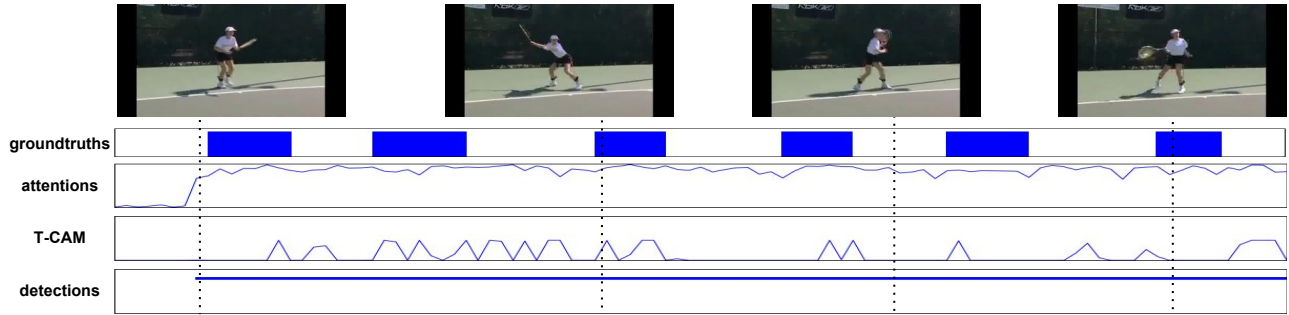
eralizability for categories with lower action instance count. We observe improvements of at least 3%AP@IoU=0.5 for 5 action categories with the lowest instance count.

Table 2 shows models trained with additional microvideos (‘Ours + MV’) improve significantly for IoU thresholds from 0.1 to 0.5, while maintaining similar performance at the higher IoU regime. This suggests the addition of microvideos allows models to recognize action instances better, but does not help with generating highly precise boundaries. These results, along with the ease of collecting and curating microvideos, presents a promising direction of using microvideos as a weakly-supervised training supplement for actional localization.

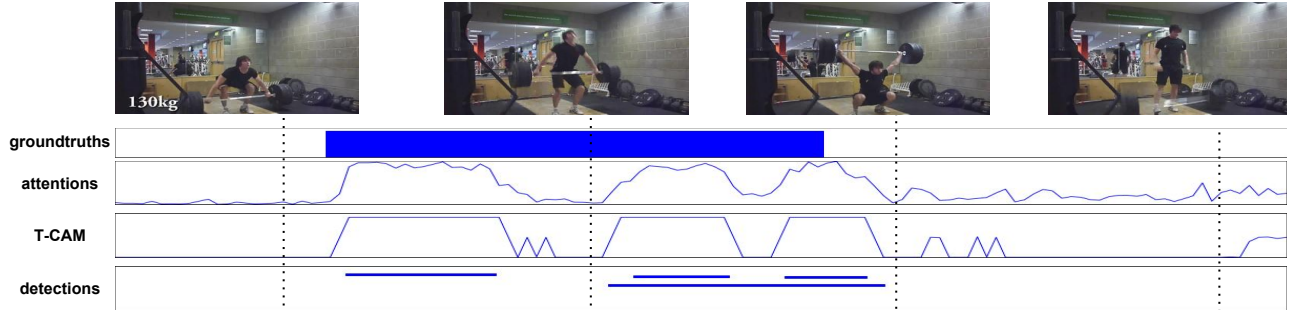
Failure modes Figure 5 examines current failure modes of our approach. Figure 5a shows multiple action instances happening close to each other, with little or no background

between them. When little background happens between actions, the model fails to correctly split the actions. Figure 5b shows an example of composite actions *CleanAndJerk*. The person performing these action usually stands still between these actions, hence the model breaks this into two components. In Figure 5c, we see another difficulty, namely the subjectivity of boundary annotations. In training videos, the action of ‘BasketballDunk’ usually involves someone running to the basket, jumping and dunking the ball. Human annotations however just consider the last piece of the action as the ground-truth. It is challenging for weakly-supervised methods to find the correct human-agreed boundaries in this case, limiting performance in higher IoU regimes. For a better visual sense of these failure cases, we refer the reader to our supplementary materials.

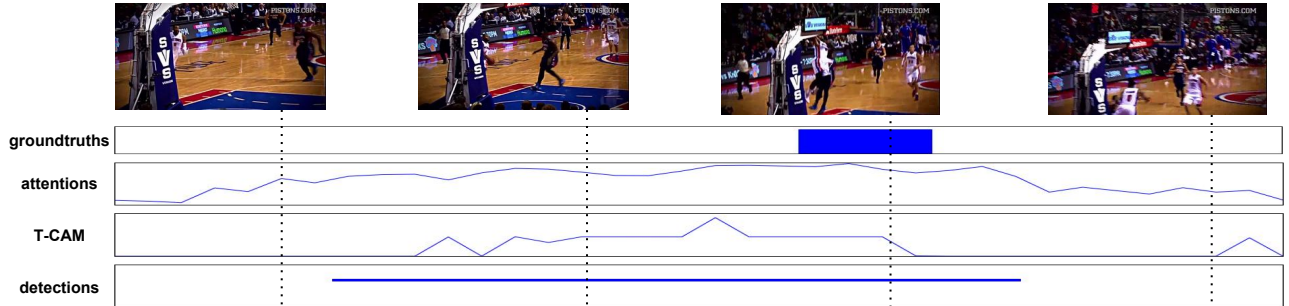
Discussion Without sparsity loss, the majority of STPN’s attention weights λ_t remain close to 1, rendering them useless for detection generation. The sparsity loss forces the attention module to output more diverse values for attention weights. However, this loss in combination with video-level foreground loss encourages the model to select the smallest number of frames necessary to predict the video-level labels. After a certain point in the training process, localization performance starts to deteriorate significantly as the sparsity loss continues to eliminate relevant frames. *This requires early stopping to prevent performance drop.* In contrast, our model uses top-down T-CAMs



(a) Failure due to similar background across consecutive instances (*Tennis*).



(b) Failure due to action composed of two mini-actions (*CleanAndJerk*).



(c) Failure due to subjective boundaries (*Basketball*).

Figure 5: Qualitative examples of failure cases where it is difficult to resolve action locations with only video-level supervision.

as a form of self-supervision for the attention weights. As a result, our model can simply be trained to convergence.

Conclusion We introduced a method for learning action localization from weakly supervised training data which outperforms existing approaches and even some fully supervised models. We attribute the success of this approach to building up an explicit model for background content in the video. By coupling top-down models for action with bottom-up models for clustering, we are able to learn a latent attention signal that can be used to propose action intervals using simple thresholding without the need for more complex sparsity or temporal priors on action extent. Perhaps most exciting is that the resulting model can make use of additional weakly supervised data which is readily collected online. Despite domain shift between Instagram videos and THUMOS14, we are still able to improve performance across many categories, demonstrating the power

of the weakly supervised approach to overcome the costs associated with expensive video annotation.

Acknowledgements This work was supported in part by a hardware donation from NVIDIA, NSF Grants 1253538, 1618903 and the Office of the Director of National Intelligence (ODNI), Intelligence Advanced Research Projects Activity (IARPA), via Department of Interior/Interior Business Center (DOI/IBC) contract number D17PC00345. The U.S. Government is authorized to reproduce and distribute reprints for Governmental purposes not withstanding any copyright annotation thereon. Disclaimer: The views and conclusions contained herein are those of the authors and should not be interpreted as necessarily representing the official policies or endorsements, either expressed or implied of IARPA, DOI/IBC or the U.S. Government.

References

- [1] Humam Alwassel, Fabian Caba Heilbron, and Bernard Ghanem. Action search: Spotting actions in videos and its application to temporal action localization. In *ECCV*, 2018.
- [2] Shyamal Buch, Victor Escorcia, Chuanqi Shen, Bernard Ghanem, and Juan Carlos Niebles. Sst: Single-stream temporal action proposals. In *CVPR*. IEEE, 2017.
- [3] Fabian Caba Heilbron, Joon-Young Lee, Hailin Jin, and Bernard Ghanem. What do i annotate next? an empirical study of active learning for action localization. In *ECCV*, 2018.
- [4] Yu-Wei Chao, Sudheendra Vijayanarasimhan, Bryan Seybold, David A Ross, Jia Deng, and Rahul Sukthankar. Rethinking the faster r-cnn architecture for temporal action localization. In *CVPR*, 2018.
- [5] Xiyang Dai, Bharat Singh, Guyue Zhang, Larry S Davis, and Yan Qiu Chen. Temporal context network for activity localization in videos. In *ICCV*. IEEE, 2017.
- [6] Victor Escorcia, Fabian Caba Heilbron, Juan Carlos Niebles, and Bernard Ghanem. DAPs: deep action proposals for action understanding. In *ECCV*, 2016.
- [7] Victor Escorcia, Fabian Caba Heilbron, Juan Carlos Niebles, and Bernard Ghanem. Daps: Deep action proposals for action understanding. In *ECCV*. Springer, 2016.
- [8] Gunnar Farneback. Two-frame motion estimation based on polynomial expansion. In *Scandinavian conference on Image analysis*, pages 363–370. Springer, 2003.
- [9] Dashan Gao, Vijay Mahadevan, and Nuno Vasconcelos. The discriminant center-surround hypothesis for bottom-up saliency. In *Advances in neural information processing systems*, pages 497–504, 2008.
- [10] Jiyang Gao, Zhenheng Yang, and Ram Nevatia. Cascaded boundary regression for temporal action detection. *BMVC*, 2017.
- [11] Jiyang Gao, Zhenheng Yang, Chen Sun, Kan Chen, and Ram Nevatia. Turn tap: Temporal unit regression network for temporal action proposals, 2017.
- [12] Chunhui Gu, Chen Sun, Sudheendra Vijayanarasimhan, Caroline Pantofaru, David A Ross, George Toderici, Yeqing Li, Susanna Ricco, Rahul Sukthankar, Cordelia Schmid, et al. Ava: A video dataset of spatio-temporally localized atomic visual actions. *CVPR*, 2018.
- [13] F. C. Heilbron, V. Escorcia, B. Ghanem, and J. C. Niebles. ActivityNet: a large-scale video benchmark for human activity understanding. In *CVPR*, 2015.
- [14] Fabian Caba Heilbron, Juan Carlos Niebles, and Bernard Ghanem. Fast temporal activity proposals for efficient detection of human actions in untrimmed videos. In *CVPR*, 2016.
- [15] Y.-G. Jiang, J. Liu, A. Roshan Zamir, G. Toderici, I. Laptev, M. Shah, and R. Sukthankar. THUMOS challenge: Action recognition with a large number of classes, 2014.
- [16] Nebojsa Jojic and Brendan J Frey. Learning flexible sprites in video layers. In *CVPR*, 2001.
- [17] Will Kay, Joao Carreira, Karen Simonyan, Brian Zhang, Chloe Hillier, Sudheendra Vijayanarasimhan, Fabio Viola, Tim Green, Trevor Back, Paul Natsev, et al. The kinetics human action video dataset. *arXiv preprint arXiv:1705.06950*, 2017.
- [18] Alberto Montes, Amaia Salvador, Santiago Pascual, and Xavier Giro-i Nieto. Temporal activity detection in untrimmed videos with recurrent neural networks. In *1st NIPS Workshop on Large Scale Computer Vision Systems (LSCVS)*, 2016.
- [19] Phuc Nguyen, Ting Liu, Gautam Prasad, and Bohyung Han. Weakly supervised action localization by sparse temporal pooling network. *CVPR*, 2018.
- [20] Phuc Xuan Nguyen, Gregory Rogez, Charless Fowlkes, and Deva Ramanan. The open world of micro-videos. *CVPR BigVision Workshop*, 2016.
- [21] Sujoy Paul, Sourya Roy, and Amit K Roy-Chowdhury. W-talc: Weakly-supervised temporal activity localization and classification. *ECCV*, 2018.
- [22] Shaoqing Ren, Kaiming He, Ross Girshick, and Jian Sun. Faster r-cnn: Towards real-time object detection with region proposal networks. In *Advances in neural information processing systems*, pages 91–99, 2015.
- [23] Alexander Richard and Juergen Gall. Temporal action detection using a statistical language model. In *CVPR*, 2016.
- [24] Zheng Shou, Jonathan Chan, Alireza Zareian, Kazuyuki Miyazawa, and Shih-Fu Chang. CDC: convolutional-deconvolutional networks for precise temporal action localization in untrimmed videos. *CVPR*, 2017.
- [25] Zheng Shou, Hang Gao, Lei Zhang, Kazuyuki Miyazawa, and Shih-Fu Chang. Autoloc: Weakly-supervised temporal action localization. *ECCV*, 2018.
- [26] Zheng Shou, Dongang Wang, and Shih-Fu Chang. Temporal action localization in untrimmed videos via multi-stage cnns. In *CVPR*, 2016.
- [27] Gunnar A. Sigurdsson, Gül Varol, Xiaolong Wang, Ali Farhadi, Ivan Laptev, and Abhinav Gupta. Hollywood in homes: Crowdsourcing data collection for activity understanding. In *ECCV*, 2016.
- [28] Gurkirt Singh and Fabio Cuzzolin. Untrimmed video classification for activity detection: submission to ActivityNet challenge. *arXiv preprint arXiv:1607.01979*, 2016.
- [29] Krishna Kumar Singh and Yong Jae Lee. Hide-and-seek: Forcing a network to be meticulous for weakly-supervised object and action localization. In *ICCV*, 2017.
- [30] Limin Wang, Yuanjun Xiong, Dahua Lin, and Luc van Gool. Untrimmednets for weakly supervised action recognition and detection. In *CVPR*, 2017.
- [31] R. Wang and D. Tao. UTS at Activitynet 2016. *ActivityNet Large Scale Activity Recognition Challenge*, 2016.
- [32] Huijuan Xu, Abir Das, and Kate Saenko. R-C3D: region convolutional 3d network for temporal activity detection. In *ICCV*, 2017.
- [33] Huijuan Xu, Abir Das, and Kate Saenko. R-c3d: region convolutional 3d network for temporal activity detection. In *ICCV*, 2017.
- [34] Serena Yeung, Olga Russakovsky, Greg Mori, and Li Fei-Fei. End-to-end learning of action detection from frame glimpses in videos. In *CVPR*, 2016.

- [35] Jun Yuan, Bingbing Ni, Xiaokang Yang, and Ashraf A Kasim. Temporal action localization with pyramid of score distribution features. In *CVPR*, 2016.
- [36] Zehuan Yuan, Jonathan C Stroud, Tong Lu, and Jia Deng. Temporal action localization by structured maximal sums. In *CVPR*, 2017.
- [37] Yue Zhao, Yuanjun Xiong, Limin Wang, Zhirong Wu, Xiaoou Tang, and Dahua Lin. Temporal action detection with structured segment networks. *ICCV*, 2017.
- [38] Bolei Zhou, Aditya Khosla, Agata Lapedriza, Aude Oliva, and Antonio Torralba. Learning deep features for discriminative localization. In *CVPR*, 2016.